

Kramers Equation Algorithm with Kogut-Susskind Fermions on Lattice

S. Basak * and Asit K. De †

Theory Group, Saha Institute of Nuclear Physics,
1/AF Salt Lake, Calcutta - 700 064, India

Abstract

We compare the performance of the Kramers Equation Monte Carlo (KMC) Algorithm with that of the Hybrid Monte Carlo (HMC) algorithm for numerical simulations with dynamical *Kogut-Susskind fermions*. Using the lattice Gross-Neveu model in 2 space-time dimensions, we calculate the integrated autocorrelation time of different observables at a number of couplings in the scaling region on 16^2 and 32^2 lattices while varying the parameters of the algorithms for optimal performance. In our investigation the performance of KMC is always significantly below than that of HMC for the observables used. We also stress the importance of having a large number of configurations for the accurate estimation of the integrated autocorrelation time.

Keywords: Kramers Equation Algorithm, Kogut-Susskind Fermion, Lattice Gauge Theory

*e-mail: basak@tnp.saha.ernet.in

†e-mail: de@tnp.saha.ernet.in

Introduction. Numerical simulation is employed as a significant tool in the nonperturbative investigation of lattice gauge theories. Most of the serious numerical simulations with dynamical lattice fermions have so far been carried out with the so-called Hybrid Monte Carlo (HMC) algorithm [1]. It has several virtues: it is an exact algorithm, easily implementable and reasonably efficient with a dynamical critical exponent $z = 1$ in the large trajectory limit. However, with growing demand of more realistic computations, especially in QCD, there is a genuine need to search for better algorithms. There is also some evidence [2,3] of lack of reversibility in the discretized classical equations of motion in the molecular dynamics part of the HMC. This will make the algorithm inexact. Since this will presumably be worse for larger lattice volumes, it is an unwelcome situation for future computations.

The main alternatives to HMC, available at the moment, are the local bosonic algorithm by Luescher [4] and the Kramers Equation Monte Carlo (KMC) [2,5], first introduced by Horowitz [6]. In this letter, we concentrate on the KMC algorithm which is a generalized version of the HMC algorithm and is exact. The guiding trajectory of KMC includes a dissipative term. The optimally tuned KMC also maintains a dynamical critical exponent $z = 1$, but unlike HMC, for arbitrarily short trajectory length, at least for free field theories. In practice, the trajectory length is taken to be a single time-step and this presumably would help suppress the effects of the possible lack of reversibility.

For this reason, the KMC certainly merits serious investigation and has received some attention recently [2,5,7] where KMC has been applied to QCD with the gauge group $SU(2)$ and to 1+1 dimensional Gross-Neveu model. The general result of these investigations is that the KMC has performed comparably with the HMC, although neither algorithm could be called clearly more efficient. Apart from the preliminary report [7], the studies used *Wilson lattice fermions*. We feel that there is a necessity for more investigation of KMC, especially with *Kogut-Susskind fermions*.

In the following we describe our investigation of the KMC algorithm using *Kogut-Susskind* or *staggered lattice fermions* on the 1+1 dimensional Gross-Neveu model.

The Gross-Neveu model. Since simulating QCD is computationally demanding, we have tested the algorithms on a simple non-gauge model which shares some properties of QCD. The Gross-Neveu (GN) model [8] in 2 space-time dimensions is asymptotically free and displays chiral symmetry breaking. Hopefully, our experience with the GN model will serve us in good stead when confronted with the real problem, QCD.

The action of the GN model on a 2-dimensional euclidean lattice can be written down as:

$$S = \frac{1}{2g^2} \sum_x \sigma^2(x) + \sum_{x,y,f} \bar{\chi}_f(x) A_{xy} \chi_f(y) \quad (1)$$

with,

$$A_{xy} = \sigma(x) \delta_{xy} + \frac{1}{2} \sum_{\mu} \zeta_{\mu}(x) \{ \delta_{y,x+\mu} - \delta_{y,x-\mu} \} \quad (2)$$

$$\zeta_1(x) = 1, \quad \zeta_{\mu}(x) = (-1)^{x_1 + \dots + x_{\mu-1}}, \quad (3)$$

where χ and $\bar{\chi}$ are the single-component Kogut-Susskind fermion fields; σ is the scalar auxiliary field; x and y are lattice sites and f is a flavor index. If n_f represents the number

of fermion flavors on the lattice, the number of flavors in the continuum limit is $2n_f$. The lattice spacing is taken to be unity. We note that the fermion matrix A_{xy} is real and independent of flavor.

The above action is the most naive transcription of the GN model on a lattice. No improvement to reduce lattice artifacts has been used and the σ -term in the fermion matrix A_{xy} is taken to be single-site. However, this should be enough for our purpose.

Implementation of the algorithms. We start by writing the classical Hamiltonian

$$H = \sum_{sites} \left[\frac{1}{2g^2} \sigma^2 + \frac{1}{2} p^2 + \sum_f \Phi_f^\dagger (A^\dagger A)^{-1} \Phi_f \right] \quad (4)$$

which evolves the system in the fictitious time τ according to the Hamilton's equations in the HMC algorithm. The Φ fields above are the usual pseudofermionic fields, p 's are the momenta conjugate to σ and are initially obtained from respective gaussian distributions as suggested by the quadratic terms in Φ and p in H . The initial configuration of σ and p are evolved in τ according to the Hamilton's equations of motion in HMC while Φ 's are kept fixed. The Hamilton's equations are integrated in discrete steps of $\delta\tau$ using the leapfrog scheme for N_{md} steps to complete a molecular dynamics trajectory at the end of which an accept/reject step is performed. This is well known and the details of the HMC algorithm can be found in many excellent reviews and articles.

The KMC involves the modification where a term proportional to momenta p is added to the momenta itself in each trajectory,

$$\pi_i = e^{-\gamma\delta\tau} p_i + \sqrt{1 - e^{-2\gamma\delta\tau}} \eta_i \quad (5)$$

where η_i is a Gaussian noise with zero mean and unit variance and γ is a tunable parameter. The subscript i refers to the number of trajectory. The leap-frog integration is performed over a single molecular dynamics step ($N_{md} = 1$):

$$\begin{aligned} \pi_i(\delta\tau/2) &= \pi_i(0) + \frac{\delta\tau}{2} F(\sigma_i(0)), \\ \sigma_{i+1}(\delta\tau) &= \sigma_i(0) + \delta\tau \pi_i(\delta\tau), \\ \pi_{i+1}(\delta\tau) &= \pi_i(\delta\tau/2) + \frac{\delta\tau}{2} F(\sigma_{i+1}(\delta\tau)), \end{aligned}$$

with the force at the site x

$$F_x(\sigma_i) = -\frac{1}{g^2} \sigma_i(x) + \sum_f \left[\Omega_f^\dagger(x) \xi_f(x) + \xi_f^\dagger(x) \Omega_f(x) \right], \quad (6)$$

where Ω and ξ are given by, $(A^\dagger A)\xi_f = \Phi_f$, $\Omega_f = A\xi_f$.

After this a Metropolis accept/reject test with acceptance probability $P(\sigma_i, \pi_i \rightarrow \sigma_{i+1}, \pi_{i+1}) = \min\{1, e^{H(\sigma_i, \pi_i) - H(\sigma_{i+1}, \pi_{i+1})}\}$ is performed. If the new configuration $(\sigma_{i+1}, \pi_{i+1})$ is accepted, we start again from Eq. 5 with $p_{i+1} = \pi_{i+1}$, and if rejected, we set $\sigma_{i+1} = \sigma_i$, $p_{i+1} = -\pi_i$ and try again starting from Eq. 5. It is important to negate the momenta in case of rejection to guarantee exactness of the algorithm. Momenta p and the pseudofermionic fields Φ are refreshed after every k -trajectories.

Here γ and k are tunable parameters. In the limit $\gamma = \infty$ and $k = 1$ KMC reduces to HMC algorithm with $N_{md} = 1$.

Autocorrelation time. A good measure of how correlated are the configurations generated by HMC and KMC, for a particular observable, is the integrated autocorrelation time for that observable. For either algorithm, we have measured it for σ and the fermion propagator.

Using the *window* method suggested by Sokal [9], an estimator for the integrated autocorrelation time τ_{int} of some observable θ can be expressed as

$$\tau_{int}(T_{cut}) = \frac{1}{2} + \sum_{t=1}^{T_{cut}} \frac{C_{\theta}(t)}{C_{\theta}(0)}. \quad (7)$$

where $C_{\theta}(t)$, the unnormalized autocorrelation function, can be estimated by the following expression:

$$C_{\theta}(t) = \frac{1}{n - |t|} \sum_{i=1}^{n-|t|} (\theta_i - \bar{\theta})(\theta_{i+t} - \bar{\theta}). \quad (8)$$

θ_i is the average value of θ for the i -th configuration and $\bar{\theta}$ is obtained by averaging over the θ_i 's. n is the total number of configurations, a large number, but obviously finite.

In the above, the factor of $1/2$ is purely a convention and T_{cut} is a cut-off for the sum, to be chosen judiciously so that one strikes a balance between noise (in case T_{cut} is too large) and bias (in case T_{cut} is too small) in the estimation of τ_{int} . In short, the recommendation of ref. [9] is to take $T_{cut} \geq c\tau_{int}$, where c is a number between 4 and 10 depending on the system and $n \gg \tau_{int}$.

If one plots τ_{int} as a function of T_{cut} for a given observable, one can read off the value of τ_{int} from a plateau region where τ_{int} is independent of T_{cut} . Such plateau regions are indeed obtained and will be discussed when results are presented in the following.

Performance tests. The numerical simulations were carried out on 16^2 and 32^2 lattices using $n_f = 4$. For HMC, we maintained $N_{md}\delta\tau \sim 1$ and the ansatz for the input vector for the matrix inversion at each time-step within the molecular dynamics trajectory was simply taken to be the result-vector of the matrix-inversion of the previous time-step. For both algorithms, the parameters of the guiding Hamiltonian were not tuned for optimal performance and the conjugate gradient inverter was used for fermion matrix inversions without any preconditioning. Preconditioning does not seem to work anyway for Kogut-Susskind fermions. The parameters of the algorithms were always tuned so as to keep the acceptance rate above 90%.

We tried both cold and hot starts, but for the production runs we always used cold starts for both algorithms. At each set of parameters we typically used 1000 iterations in HMC and 16000 iterations in KMC for equilibration. As we will see, these numbers are substantially larger than $20\tau_{int}$, suggested by [9], for the observables of interest.

We determined the scaling region by plotting $\langle\sigma\rangle$ as a function of $1/g^2$. The scaling window is between $g = 0.55 - 0.45$ for 16^2 lattice and gets slightly beyond 0.45 for 32^2 . For the investigation of autocorrelation times, we collected data at various values of the coupling g always remaining within the scaling window.

For HMC, we varied $\delta\tau$ from 0.033 to 0.05 always maintaining $N_{md}\delta\tau \sim 1$. For each coupling we tried to find the best value for the ratio $r = a/2\tau_{int}$ where a is the acceptance rate. The bigger the ratio, the better is the performance. On 16^2 lattice at $g = 0.5$ this is obtained at $\delta\tau = 0.04$ for the observable $\langle\sigma\rangle$ and roughly also for the fundamental fermion propagator. In Fig.1a we have plotted τ_{int} versus T_{cut} for each of these observables for 16^2 lattice. The lower curve is for the fermion propagator, and to be specific, we have presented the autocorrelation data for zero-spatial-momentum propagator at time separation of 3. For the subsequent plots of fermion propagator autocorrelation, we will use this particular propagator. For a given T_{cut} , we have measured τ_{int} from each of 15 segments, each segment-size being 1500 configurations for $\langle\sigma\rangle$ and 1000 for the fermion propagator. The errors on the τ_{int} data represents the statistical error from the 15 values for each T_{cut} . In subsequent plots the same procedure will be followed, although the segment-size and the number of segments will be changed appropriately. From Fig.1a, one can easily find a plateau region from which τ_{int} can be read off. One sees also that the fermion propagator has significantly smaller integrated autocorrelation time.

For a reasonably accurate determination of τ_{int} we found it absolutely essential to have large segment sizes ($\sim 1000\tau_{int}$). With smaller segment sizes we have found it difficult to find the plateau because of excessive noise. As a general observation, we have noticed that the value of τ_{int} , if at all one can read it off, is always lower when the segment-size is small. In HMC, for both 16^2 and 32^2 lattices, we have actually determined τ_{int} at least for $\langle\sigma\rangle$ for a host of other values of $g = 0.52, 0.48, 0.46$ with segment-size of 100 configurations and have rough estimation of autocorrelations at those couplings too. For KMC, the ill-effects of having small segment sizes were more dramatic.

For KMC, we varied $\delta\tau$ from 0.033 to 0.05 on 16^2 and 32^2 lattices and also varied the parameters γ and k . Within our range of the parameters the near-optimal choice for the ratio r at $g = 0.5$ was $\delta\tau = 0.04, \gamma = 1.5, k = 4$ on 16^2 lattice and in Fig.1b we present the corresponding autocorrelation time data (later, we found that by increasing k to 8, it was possible to enhance the performance of KMC somewhat, and thus our choice of parameters is not quite optimal). Large statistics was required to produce the figure. The segment-size was 72,000 configurations for fermion propagators and 100,000 for $\langle\sigma\rangle$, with 5 such segments for each observable. Once again, nice plateau regions were found for τ_{int} . The propagators are again less correlated, but the values of τ_{int} for either observable in the plateau region are orders of magnitude higher than those obtained in Fig.1a for HMC. The acceptance rates are usually always higher for KMC, but the huge discrepancy in the autocorrelations, even for observables like the propagators, makes the HMC significantly better in effective performance, in spite of HMC's higher overhead per trajectory (see Table 1 below).

We made a qualitative estimate of the higher overhead of HMC over KMC per trajectory for all our runs. Ratio of total number of conjugate gradient iterations for one full trajectory of HMC to that for one trajectory of KMC (including Hamiltonian calculations in each case) gives an accurate estimate of the overhead. For the runs in Figs.1a and b, this overhead is 14.0 with 10% uncertainty. For all our runs at different couplings, lattice sizes and algorithm parameters, the HMC overhead was between 10 and 15.

To illustrate the point of having large enough segment sizes, we plot in Fig.2 again τ_{int} versus T_{cut} for $\langle\sigma\rangle$ on 16^2 lattice at $g = 0.5$ using the same set of parameters, but this time using 6 segments each of size 1000 configurations only. Please note the τ_{int} -scale of Fig.2 as

compared to that of Fig.1b. There is only a rough hint of a plateau in Fig.2 and the data is very noisy. Also, the actual value of τ_{int} at the anticipated plateau region of Fig.2 is about half of that in Fig.1b.

In KMC we have investigated integrated autocorrelation times at various other couplings, *viz.*, $g = 0.52, 0.48, 0.46$ with $\gamma = 1.5, \delta\tau = 0.04$ and $k = 4$ on both 16^2 and 32^2 lattices, however, with smaller statistics as in Fig.2 and could estimate τ_{int} for the observables only very roughly. Still in each case the autocorrelation time was found to be orders of magnitude higher than the corresponding values with HMC, as shown in Table 2 presented later.

On 16^2 lattice, with $k = 4$ and $\delta\tau = 0.04$ we have also varied the parameter γ from 0.5 to 2.0 in intervals of 0.5 for a number couplings g from 0.52 to 0.46. The autocorrelation time determinations could only be done with relatively small statistics. The optimal γ was found in each case to be qualitatively consistent with the free theory estimate of $1/m_s$ where m_s is the smallest mass of the theory. As a result the optimal γ shifted towards higher values as the coupling g was lowered with all other parameters kept fixed.

In addition to $k = 4$, we have performed similar autocorrelation investigations at $k = 8$ on 16^2 lattice using $\gamma = 1.5, \delta\tau = 0.04$ at couplings $g = 0.50, 0.46$. By increasing the value of k , there was an indication in our data of an enhancement of the ratio r at the lower coupling. Still it was too little to boost it up on par with HMC.

In Table 1 we present the values of τ_{int} and the ratio r for $\langle\sigma\rangle$ and the fermion propagator at $g = 0.5$ on 16^2 lattice in both HMC and KMC for the data shown in Fig.1a and Fig.1b. Put together with higher overhead for HMC (discussed earlier), table 1 then indicates that HMC is about 9.5 and 7.5 times more efficient than KMC respectively for $\langle\phi\rangle$ and for fermion propagator. Table 2 collects some results from small statistics runs on both 16^2 and 32^2 lattices at a few other couplings in the scaling region. The data at $g = 0.46$ on 16^2 lattice has higher statistics than the rest in Table 2, as evident from smaller errors. The KMC data on 32^2 lattice are the most inaccurate and the values of τ_{int} are likely to be significantly below their actual values.

Conclusions. In our investigation of relative performances of HMC and KMC algorithms with dynamical *Kogut-Susskind fermions* on a simple 2-dimensional Gross-Neveu model, we found that the HMC was significantly more efficient in producing uncorrelated configurations than the KMC. When other similar investigations [2,5] with *Wilson fermions* did not find a significant difference of performance between the two algorithms, our results indicate, taking into account the higher overhead per trajectory of the HMC which in our case was always between 10 and 15, a difference of about *an order of magnitude* for all combinations of parameters and couplings we tried. How much of our conclusion would carry over to QCD with Kogut-Susskind fermions is an open question.

Our choice of parameters for KMC might not have been optimal in all cases, but it becomes apparent that KMC requires a lot of tuning and our investigation shows that we were unable to find a set of parameters which could make KMC even remotely competitive.

We emphasize again the importance of having a large number of configurations for the estimation of τ_{int} . Without it, the data is not just noisy, the roughly estimated τ_{int} is well below the actual value.

REFERENCES

- [1] S. Duane, A.D. Kennedy, B.J. Pendleton and D. Roweth, Phys. Lett B195 (1987) 216.
- [2] K. Jansen and C. Liu, Nucl. Phys. B453(1995) 375.
- [3] K. Jansen and C. Liu, hep-lat/9708017.
- [4] M. Luescher, Nucl. Phys. B418 (1994) 637; P. de Forcrand, Nucl. Phys. B (Proc. Suppl.) 47 (1996) 228.
- [5] M. Beccaria, G. Curci and L. Galli, Phys. Rev. D49 (1994) 2590.
- [6] A.M. Horowitz, Phys. Lett. B156 (1985) 89; Nucl. Phys. B280 (1987) 510; Phys. Lett. B268 (1991) 247.
- [7] M.E. Berbenni-Bitsch, A.P. Gottlob, S. Meyer and M. Puetz, Nucl. Phys. B (Proc. Suppl.) 53 (1997) 965.
- [8] D.J. Gross and A. Neveu, Phys. Rev. D10 (1974) 3235
- [9] N. Madras and A.D. Sokal, J. Stat. Phys. 50 (1988) 109

FIGURE CAPTIONS

Fig. 1. Integrated autocorrelation times for $\langle\sigma\rangle$ and fermion propagator (zero spatial momentum with time-separation 3) at $g = 0.5$ on 16^2 lattice for (a) HMC with $\delta\tau = 0.04$, (b) KMC with $\delta\tau = 0.04$, $\gamma = 1.5$, $k = 4$.

Fig. 2. Low statistics data on τ_{int} for $\langle\sigma\rangle$ in KMC at $g = 0.5$ on 16^2 lattice with the same set of parameters as in Fig. 1b.

TABLE CAPTIONS

Table 1. τ_{int} and r for $g = 0.50$ obtained on 16^2 lattice (HMC: $\delta\tau = 0.04$; KMC: $\delta\tau = 0.04$, $\gamma = 1.5$, $k = 4$).

Table 2. τ_{int} and r for various g obtained on 16^2 and 32^2 lattice for $\langle\sigma\rangle$ (HMC: $\delta\tau = 0.04$; KMC: $\delta\tau = 0.04$, $\gamma = 1.5$, $k = 4$).

TABLES

Algorithm	$\langle\sigma\rangle$		<i>propagator</i>	
	τ_{int}	r	τ_{int}	r
HMC	1.72(28)	29(5)	0.83(11)	63(8)
KMC	228(27)	0.22(2)	83(6)	0.60(5)

TABLE 1.

		$g = 0.52$		$g = 0.48$		$g = 0.46$	
		τ_{int}	r	τ_{int}	r	τ_{int}	r
16^2	HMC	1.22(48)	45(18)	1.30(45)	40(13)	1.05(20)	48(9)
	KMC	128(64)	0.50(25)	108(26)	0.47(11)	138(23)	0.36(6)
32^2	HMC	1.47(38)	33(8)	1.47(50)	33(11)	1.56(31)	30(6)
	KMC	124(97)	0.84(66)	142(107)	0.63(47)	–	–

TABLE 2.

FIGURES

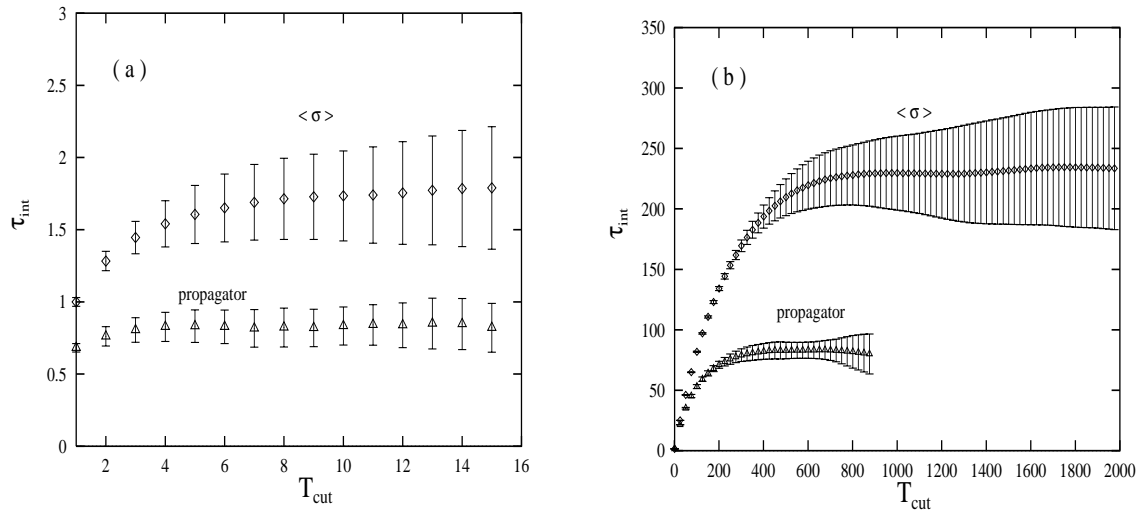


FIG. 1.

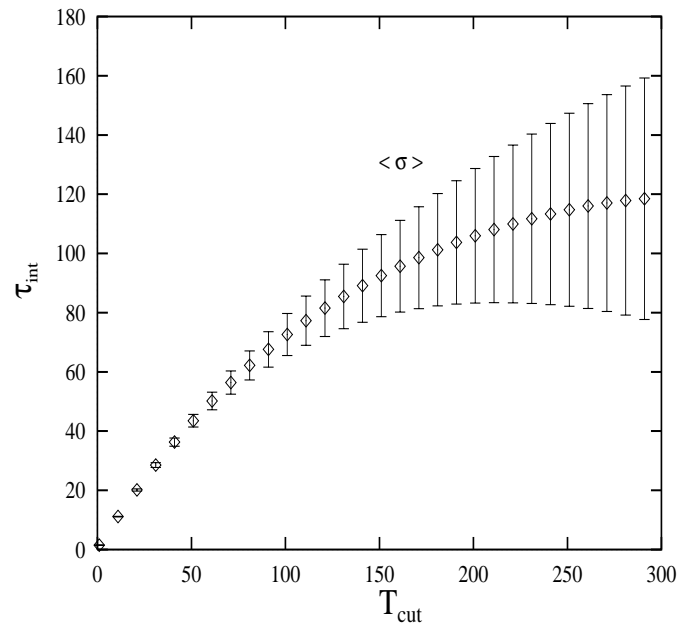


FIG. 2.